Background Correction in First-Pass Radionuclide Angiography: Comparison of Several Approaches

Rami Gal, Raymond P. Grenier, Donald H. Schmidt, and Steven C. Port

Nuclear Cardiology Laboratory, Mount Sinai Medical Center, University of Wisconsin Medical School, Milwaukee Clinical Campus, Milwaukee, Wisconsin

This study was designed to test the comparative accuracy of several commonly used background correction techniques in first-pass radionuclide angiography (FPRNA). Thirty patients underwent FPRNA and single plane contrast angiography (CA) within 1 hr of each other. The left ventricular ejection fractions (LVEF) calculated from the different background subtraction approaches to FPRNA were compared to the CA LVEF. When applied to a representative cycle, a horseshoe-shaped background region of interest (BKROI) underestimated LVEF ($p < 0.005$, $r = 0.91$, s.e.e. = 0.06) while a ring shaped BKROI adjusted at end-systole for aortic valve motion insignificantly overestimated LVEF (p = NS, $r = 0.91$, s.e.e. = 0.07). A lung background approach applied to a representative cycle gave the best correlation with CA (p = NS, $r = 0.96$, s.e.e. = 0.04). Without using a representative cycle, time-activity curves from a horseshoe-shaped BKROI and the LV ROI were created and the LV curve was normalized to the peak counts in the BKROI curve. LVEF calculated from the normalized curve correlated favorably with CA LVEF (p = NS, $r = 0.91$, s.e.e. = 0.08). The influence of some recently described improvements in representative cycle generation are also documented.

J Nucl Med 27:1480–1486, 1986

Among indices of left ventricular function, the ejection fraction has been shown to be the most useful prognostic measurement (*1,2*). We and others have previously demonstrated a good correlation between first-pass radionuclide angiographic left ventricular ejection fraction LVEF and contrast angiographic LVEF (*3–5*). The calculation of the radionuclide LVEF is extremely dependent on the method used for background subtraction. However, few comparisons of the various background approaches to first-pass radionuclide angiography have been made using the same gamma camera/computer system (*5,6*). In this study, we compared the LVEF calculations using several commonly used background subtraction techniques to the results of contrast angiography. In addition, the influence of some newly described improvements in first-pass data processing (*3*) on the results from the different background techniques was examined.

Received Nov. 5, 1985; revision accepted Mar. 21, 1986.

For reprints contact: Steven C. Port, MD, Mount Sinai Medical Center, P.O. Box 342, Milwaukee, WI 53201.

PATIENTS AND METHODS

Patient Population

Between September 26, 1984 and December 2, 1984, 30 randomly selected patients were studied. There were 23 men and seven women ranging in age from 45–76 yr (mean 60.2). Each patient was in normal sinus rhythm at the time of study. According to the results of contrast angiography (CATH), 27 patients had coronary artery disease, two had valvular heart disease, and one had no detectable heart disease.

Study Protocol

All first-pass radionuclide angiography (FPRNA) was performed in the holding area of the catheterization laboratory, after premedication and immediately preceding the catheterization. All studies were acquired at rest, in the supine position, using a 30° right anterior oblique view. Twenty-five to thirty millicuries of technetium-99m diethylenetriaminepentaacetic acid [^{99m}Tc]DTPA were injected into an external jugular or medial antecubital vein. Imaging was performed using a single crystal small field-of-view portable gamma camera and computer*. For each study, 30 sec of data were recorded in frame mode using a frame time of 0.03 sec 32 × 32 pixel matrix. Data were collected on the hard disk and then stored on a floppy disk for subsequent processing.

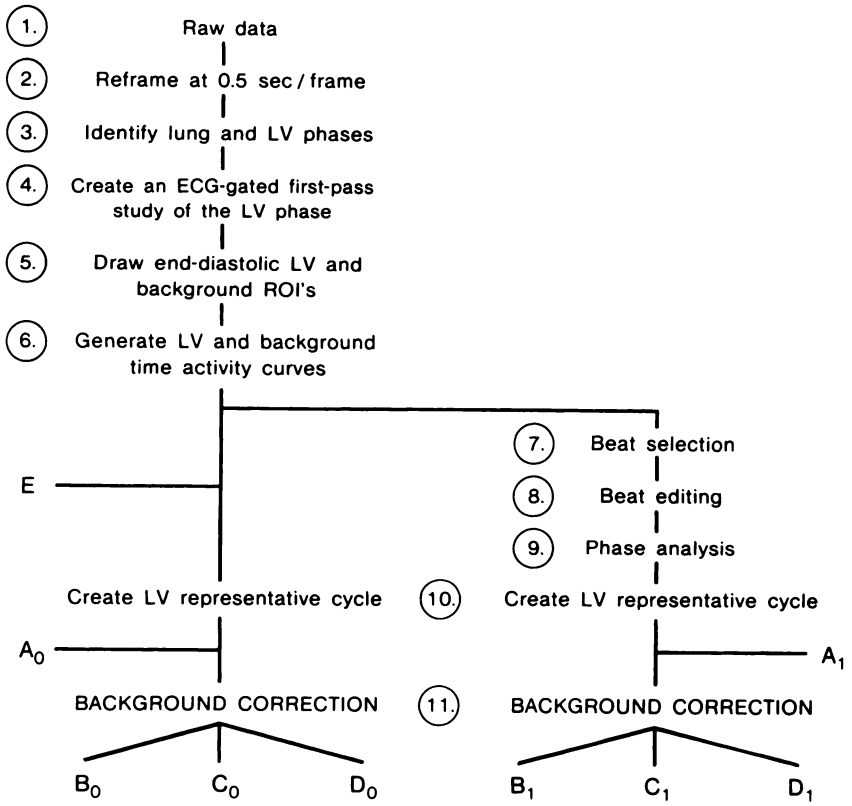

FIGURE 1
Outline of first-pass data processing

Radionuclide Data Processing

An outline of the data processing is shown in Fig. 1. The steps in data processing that were common to all methods led to the generation of time activity curves from an end-diastolic left ventricular region of interest (LV ROI) and from a background area. From the time activity curve of the LV ROI, a representative cycle was generated using frame counts rather than the ECG as criteria for selection of end-diastolic frames. That representative cycle (step 10, Fig. 1) was then used for four ejection fraction calculations, A_0, B_0, C_0, and D_0.

Method A_0 calculated LVEF from the representative cycle without any correction for background.

Method B_0 used a horseshoe-shaped background that was fitted around the apex of the end-diastolic LV image. The horseshoe-shaped ROI encompassed 285° of a circle, was 1 pixel wide and spaced 1 pixel away from the LV ROI (Fig. 2A). Average counts/pixel in the horseshoe were subtracted from each pixel in the LV ROI for each frame of the representative cycle.

Method C_0 applied a 1-pixel wide circular or ring-shaped background ROI around the end-diastolic LV ROI. The same size and shape ring was created around the end-systolic LV ROI taking care to avoid the ascending aorta (Fig. 2B). End-diastolic LV counts were corrected by subtracting the average counts/pixel in the end-diastolic ring and end-systolic LV counts were similarly corrected using the end-systolic ring.

Method D_0 used a number of "lung phase" frames (frames prior to the LV phase) equal to the number of beats in the representative cycle. These frames were summed and then multiplied by a background washout factor. The washout factor was determined from the ratio between extra-cardiac ROI counts measured in the operator chosen "lung phase frame" to the extra-cardiac ROI counts in an end-diastolic frame during the LV phase. The summed background frame corrected for washout was then subtracted from all frames of the representative cycle (*3*).

Methods A_1, B_1, C_1, and D_1 are identical to A_0, B_0, C_0, and D_0, respectively, except that the background techniques are applied to a representative cycle that had undergone beat editing, beat alignment, and adjustment of the LV ROI to a phase image of the representative cycle (steps 7–9, Fig. 1). The latter modifications have been described in detail previously (*3*).

One additional method (E) was also used. Method E was based on curve arithmetic without use of a representative cycle. Time activity curves from the LV ROI and a horseshoe-shaped background ROI were generated (step 6, Fig. 1). The LV time activity curve was then normalized to the peak counts in the background time activity curve. Ejection fraction was then calculated directly as the average of the ejection fractions of the individual beats in the corrected LV time activity curve.

In methods A_0 and A_1, LVEF was calculated as ED counts − ES counts/ED counts while in all other methods, LVEF was calculated as background corrected ED counts − background corrected ES counts/background corrected ED counts.

Contrast Angiography

After measurement of left ventricular pressures, single plane contrast left ventriculography was performed in the 30° right anterior oblique view using 30–50 cc of meglumin-diatrizoate injected in the left ventricle. The ventriculogram was filmed at 60 frames/sec on 35-mm film using a 9-in. image intensifier. Selective coronary arteriography was performed in multiple views using the Judkins technique. Angiographic LVEF was

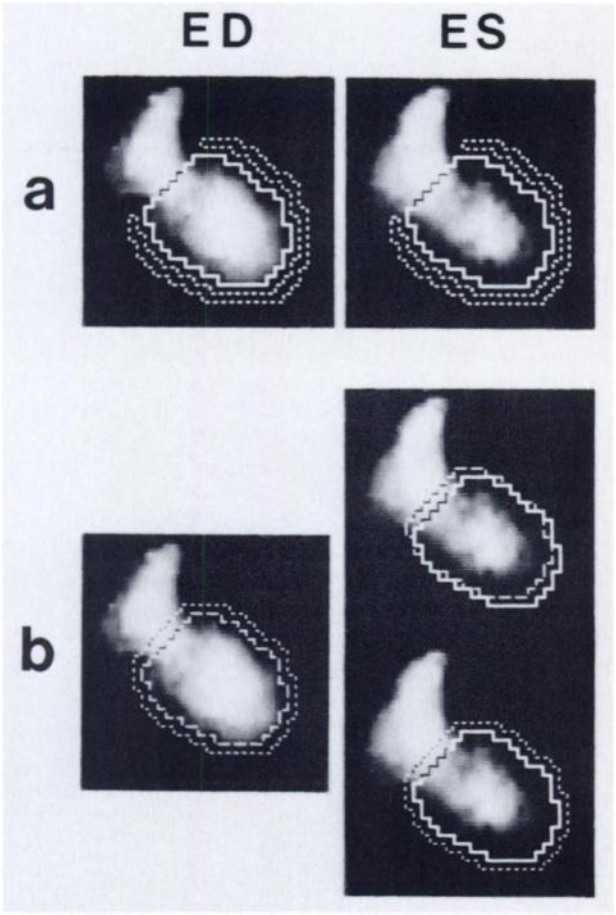

FIGURE 2
A: Example of horseshoe-shaped background method. Horseshoe-shaped ROI (dotted line) is placed around end-diastolic (ED) and end-systolic (ES) frames of representative cycle. B: On left, ring-shaped background ROI (dotted line) is placed around ED ROI. On right, upper image shows how ED ROI (broken line) appears when positioned on ES frame and how ROI is then moved (solid line) to exclude aortic activity. Lower image then shows ring-shaped background ROI placed around adjusted LV ROI on ES frame

determined for each patient using a modification of Kennedy et al. for the area-length method of Sandler et al. (*7*). Only sinus beats were selected for quantitative analysis.

Statistical Methods

The significance of differences between paired observations was determined with the Student's t-test. Correlation and linear regression analyses were performed using standard techniques. Statistical significance was determined at the $p < 0.05$ level.

RESULTS

Radionuclide Acquisition Statistics

The injection of 27 ± 2 mCi of [^{99m}Tc]DTPA resulted in a count rate of 150,112 ± 27,101 for the whole field-of-view during the right ventricular phase. The full width half maximum (FWHM) of the tracer bolus in the superior vena cava was 0.81 ± 0.22 sec. Uncorrected counts in the LV ROI averaged 42,253 ± 10,685 counts/sec at end-diastole and 27,674 ± 9,246 counts/sec at end-systole. The representative cycles were comprised of 6.5 ± 1.8 beats.

LVEF Calculations (Table 1)

The ejection fractions calculated from the representative cycles without any background subtraction were 0.31 ± 0.09 (method A_0) and 0.38 ± 0.09 (method A_1). Compared to the average CATH LVEF of 0.63 ± 0.16, the correlation coefficient, the slope of the regression line and the s.e.e. were improved by using the A_1 representative cycle instead of the A_0 representative cycle.

Methods B_0 and B_1 used horseshoe-shaped background ROIs. The calculated LVEF was 0.42 ± 0.13 for B_0 and 0.46 ± 0.13 for B_1. Both were significantly lower than the CATH LVEF ($p < 0.0001$). Methods C_0 and C_1, which used ring-shaped background areas gave much better results than the horseshoe-shaped background methods. The average LVEF was 0.65 ± 0.18 for C_0 and 0.68 ± 0.16 for C_1. Both methods gave LVEF values that were higher than the CATH LVEF results but only C_1 was significantly different ($p < 0.005$). In methods D_0 and D_1 a lung phase frame, corrected for washout, was used for background subtraction. The average LVEF was 0.56 ± 0.17 for D_0 and 0.62 ± 0.16 for D_1. The D_0 LVEF was significantly different from the CATH result ($p < 0.0005$) while the D_1 result was not.

Method E was the only method that calculated LVEF without generating a representative cycle. The average LVEF using method E was 0.65 ± 0.19 which was insignificantly different from the CATH LVEF.

Comparison of Different Background Methods (Fig. 3)

The horseshoe-shaped background applied to a representative cycle (B_0 and B_1) was the least accurate. The mean LVEF for the C_0, C_1, D_0, D_1, and E methods were all quite similar. However, the highest correlation coefficient and lowest s.e.e. were seen with the D_1 approach.

Comparison of Different Representative Cycles

The processes of beat editing, beat alignment, and adjustment of the LV ROI according to the phase image resulted in a representative cycle that gave improved correlation with the CATH result. The improvement is best demonstrated in method A_1 where there is no background subtraction. The A_1 correlation coefficient, slope of the regression line, and s.e.e. were 0.88, 0.51 and 0.04 compared with 0.83, 0.48 and 0.06 for method A_0. Similarly, the correlation coefficients were higher and the s.e.e. lower for B_1, C_1, and D_1 compared with B_0, C_0, and D_0, respectively.

DISCUSSION

First-pass radionuclide angiography has been shown to be an accurate and reproducible method for the evaluation of left ventricular function (*4–6,8*). The accuracy of FPRNA depends on two major factors. First is the quality of the raw data, which is heavily

TABLE 1
Individual Patient Data

Patient no.	Sex	Age (yr)	FPRNA LVEF*									CATH EF
			A_0	A_1	B_0	B_1	C_0	C_1	D_0	D_1	E	
1	M	54	.45	.55	.63	.67	.92	.85	.66	.76	.75	.79
2	M	68	.75	.27	.25	.28	.46	.44	.39	.45	.37	.38
3	M	58	.37	.40	.39	.41	.68	.69	.56	.60	.54	.55
4	M	58	.34	.34	.52	.52	.66	.70	.67	.69	.79	.66
5	F	59	.33	.36	.26	.39	.60	.66	.50	.51	.59	.50
6	F	62	.27	.37	.49	.50	.52	.62	.44	.60	.78	.67
7	M	59	.31	.40	.45	.49	.74	.74	.62	.64	.53	.68
8	F	51	.37	.43	.43	.55	.84	.78	.69	.73	.83	.80
9	M	69	.31	.41	.43	.47	.73	.79	.56	.69	.64	.69
10	M	57	.33	.37	.38	.42	.83	.79	.61	.65	.71	.73
11	M	61	.27	.47	.56	.56	.73	.76	.59	.65	.52	.68
12	F	55	.33	.43	.52	.59	.76	.75	.65	.70	.63	.75
13	M	48	.26	.37	.48	.62	.18	.75	.58	.76	.84	.73
14	M	65	.37	.44	.47	.52	.67	.72	.62	.67	.76	.68
15	M	55	.34	.36	.45	.47	.81	.85	.64	.73	.66	.70
16	M	52	.29	.39	.41	.50	.67	.6	.75	.82	.88	75
17	F	73	.19	.28	.33	.30	.50	.60	.28	.45	.57	.49
18	M	43	.39	.42	.50	.52	.80	.83	.68	.71	.81	.71
19	M	46	.38	.42	.41	.42	.65	.72	.68	.71	.75	.70
20	F	68	.48	.55	.58	.65	.97	.91	.59	.74	.93	.84
21	F	76	.36	.37	.49	.50	.80	.80	.50	.55	.61	.58
22	M	65	.70	.10	.70	.10	.15	.18	.6	.14	.15	.18
23	M	45	.33	.39	.34	.45	.67	.77	.81	.76	.77	.72
24	M	61	.12	.23	.19	.22	.27	.36	.25	.33	.30	.35
25	M	64	.23	.26	.28	.30	.38	.43	.34	.38	.41	.44
26	M	60	.37	.39	.42	.41	.66	.66	.66	.68	.71	.70
27	M	71	.18	.29	.16	.24	.38	.39	.36	.39	.34	.33
28	M	73	.33	.43	.54	.58	.66	.67	.62	.68	.65	.68
29	M	65	.31	.43	.41	.48	.76	.74	.66	.66	.72	.65
30	M	60	.43	.45	.60	.58	.63	.75	.74	.74	.80	.73
EF			.31	.38	.42	.46	.65	.68	.53	.62	.65	.63
r			.832	.878	.863	.910	.879	.913	.887	.959	.908	
SEE			.06	.04	.07	.06	.09	.07	.08	.04	.08	
p			<.005	<.005	<.005	<.005	NS	<.005	<.0005	NS	NS	

* A_0 and A_1—No background correction; B_0 and B_1—Horseshoe background ROI; C_0 and C_1—Ring background ROI; D_0 and D_1—Lung background; E—Curve arithmetic (horseshoe-shaped background ROI).

influenced by the count rate, the discreteness of the radionuclide bolus, and the transit time through the right heart and pulmonary circulation. Those are variables that change from patient to patient and, except for the quality of the radionuclide bolus, are largely uncontrollable. The second major factor influencing the accuracy of FPRNA is the data processing. Data processing can be divided into two main areas, generation of a representative cycle and background correction. In a previous study we described an improved approach to generating a representative cycle during FPRNA (*3*). In this study we have attempted to assess the influence of several commonly used background subtraction techniques on the accuracy of LVEF results. All of the background correction techniques used in this study have been individually validated but no attempt has ever been made (presumably due to software constraints) to compare the various methods in an effort to see if any method is significantly better than another.

Background may be defined as counts which are registered in the LV ROI but do not originate from the LV chamber. There are two major sources of LV background which have to be considered. The first is anatomic overlap from left atrium, lungs, aorta, right ventricle, and myocardium which contriute background counts to counts recorded within the LV ROI. The second is Compton scatter which consists of events which originate outside the LV ROI, but due to scatter in the LV chamber and surrounding myocardium, are registered as counts from the LV ROI. The most effective technique to control background contamination in the data is to minimize and eliminate as many sources of background as possible from the raw measurement.

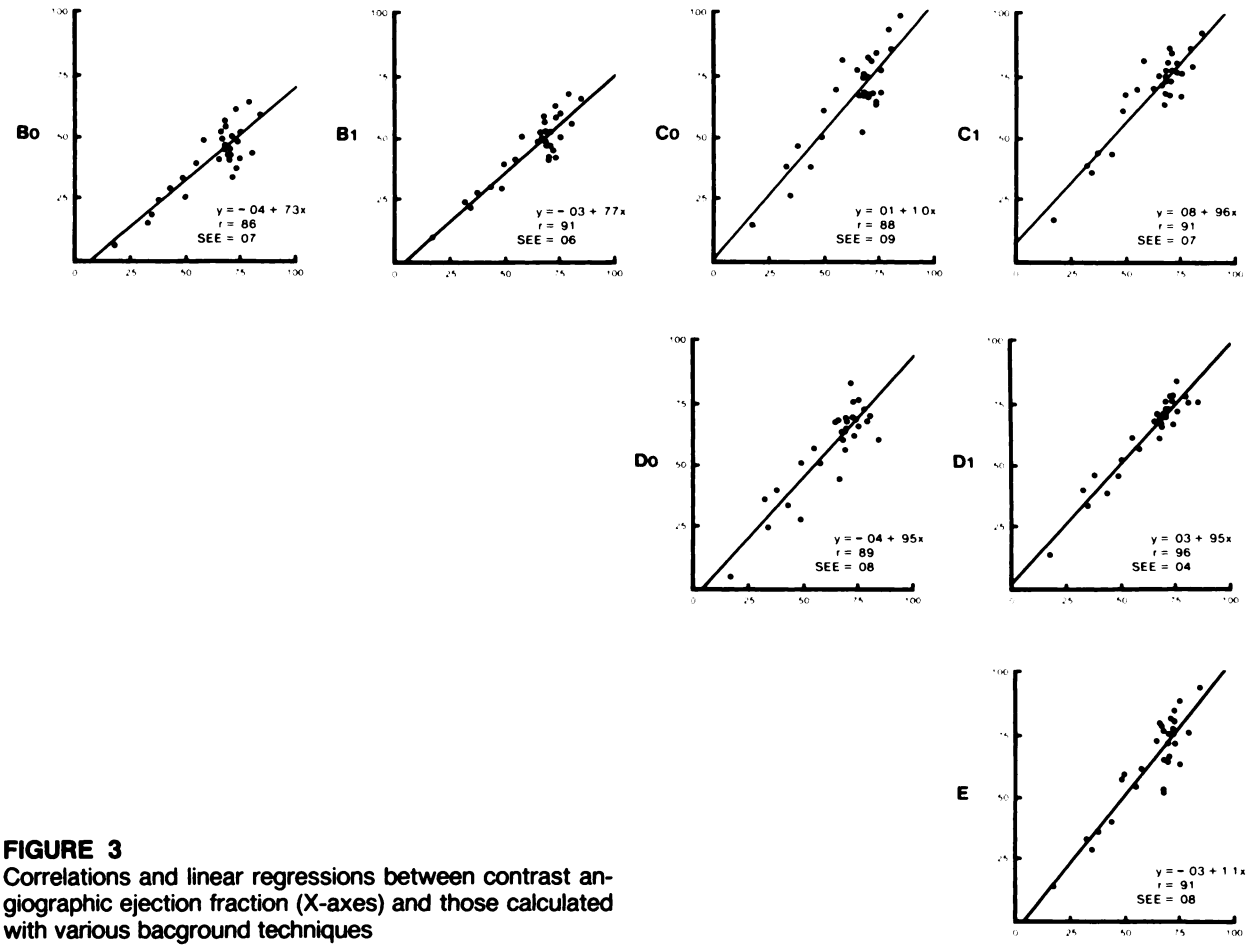

FIGURE 3
Correlations and linear regressions between contrast angiographic ejection fraction (X-axes) and those calculated with various bacground techniques

The first-pass technique by its very nature minimizes right ventricular and myocardial background counts due to timing of the left ventricular phase, which follows right ventricular clearance and precedes myocardial appearance. The right anterior oblique orientation enhances separation of the proximal aorta, descending aorta, and some of the left atrium from direct anatomic overlap with the left ventricle. That leaves the left lung, portions of the left atrium, and Compton scatter as the major sources of background counts in the left ventricular ROI. The "lung" background correction approach is a technique to correct for background due to overlap of left lung, left atrium, and Compton scatter. The use of ring or horseshoe-shaped background ROIs are approaches which use the close proximity of the background ROI to the LV ROI as a quantitative estimate of the background, especially the scatter component.

Lung Background Method

Because of its association with the multicrystal gamma camera, the "lung" method (D_0 and D_1) is probably the most widely used background correction technique in FPRNA (*4,8*). The "lung" method assumes that the distribution of activity in frames prior to the appearance of activity in the left ventricle is an accurate spatial representation of the background. In addition, a washout factor is used to account for the decrease in activity in the background region during the left ventricular phase. Previous studies have documented correlation coefficients of 0.86 to 0.95 (*4–6,8,9*) and s.e.e. of 0.06 (*4*) to 0.095 (*9*) compared with contrast angiography. In our study the lung (D_1) method produced the highest correlation coefficient (0.96) and the smallest s.e.e. (0.04) of all the background approaches.

Horseshoe and Ring Background Methods

The horseshoe (B_0 and B_1) and ring (C_0 and C_1) methods for background subtraction use manually or automatically drawn regions around the LV ROI. The width of the background region and spacing from the LV ROI vary from study to study and have not been critically evaluated. With either method the counts in the background region are normalized according to the ratio of the areas of the background to the LV ROIs. Then the normalized average counts per pixel in the background region are subtracted from each pixel in the LV ROI. Both Steele et al. (*10*) and Folland et al. (*11*) showed that a horseshoe-shaped ROI applied to time activity curves rather than representative cycles tended to underestimate the contrast angiographic results. In our study the horseshoe method applied to a

representative cycle significantly underestimated the contrast angiographic results. Most likely, that underestimation results from an under-representation of left atrial and pulmonary venous background activity in the horseshoe ROI. In contrast, the ring method obviates the latter problem but results in a tendency to overestimate the true LVEF. The overestimation probably results from the inclusion of aortic root activity in the background ROI especially at end-systole when the aortic root moves toward the apex of the ventricle. Both Schelbert et al. (*6*) and Ashburn et al. (*5*) have previously documented overestimation using the ring method applied to time activity curves. Despite the overestimation in this study, the ring method gave ejection fraction results that were much closer to the contrast values than did the horseshoe (B) approach. We believe that the concentration of activity in the left atrium and pulmonary veins during the first half of the LV phase (RP Grenier, unpublished observations) accounts for the better results, as well as repositioning of the LV ROI in ES (compared to previous location in ED) obtained with the ring ROI compared with the horseshoe ROI. Interestingly, when we used a horseshoe ROI to generate a time activity curve which was then used to correct the time activity curve of the LV ROI (method E), there was no underestimation of the contrast LVEF. Hence, there is a disparity between the results of applying a horseshoe-shaped background ROI to a representative cycle and of using the same horseshoe-shaped background ROI to normalize an LV time activity curve without use of a representative cycle. That discrepancy can best be explained by the higher background subtracted at end-systole using the curve normalization approach. In the latter, the cyclic fluctuations in background activity from ED to ES are smoothed away, whereas in the representative cycle approach there is always less background subtracted at ES than at ED. The lower background at ES is presumbly due to a decrease in the scatter component as a result of the smaller LV volume.

Importance of the Representative Cycle

As mentioned previously, the lung background approach applied to a representative LV cycle gave the best results compared with contrast angiography. Furthermore, the lung background approach corrects the images for anatomic overlap during the entire cardiac cycle thus improving wall motion analysis (*3*). Clearly, when one has the software capability to generate a representative cycle it is the procedure of choice. In addition, the method of generating the representative cycle is important as evidenced by the improved correlations using A_1, B_1, C_1, and D_1 compared to A_0, B_0, C_0, and D_0 in this study. The main reason for including A_0 and A_1 (no background subtraction) was to document the improved correlation with the contrast results obtained by using the newly developed method of creating the representative cycle without even considering background. The advantages of the newer method are the operator interaction in individual beat selection and beat editing as well as use of a phase image for adjustment of the LV ROI when necessary.

In summary, our results suggest that processing of FPRNA data should make use of a representative cycle if possible and that a lung background approach applied to a representative cycle generated in a manner described above gives the most favorable comparison with results of contrast angiography. If software for generating a representative cycle is not available, then correcting the LV time activity curve with a normalized time activity curve from a horseshoe-shaped background ROI provides acceptable ejection fraction results except for a higher standard error of the estimate.

FOOTNOTE

* Elscint, Inc., Boston, MA (Apex 215).

ACKNOWLEDGMENTS

The authors gratefully acknowledge Mr. Eitan Shaham and Dr. Karol Herskovicci of Elscint, Inc. for their expert programming assistance, and Ms. Jean Ciske for manuscript preparation.

REFERENCES

1. Cohn PF, Gorlin R, Cohn LH, et al: Left ventricular ejection fraction as a prognostic guide in surgical treatment of coronary and valvular heart disease. *Am J Cardiol* 34:136–141, 1974
2. Pryor DB, Harrell FE Jr., Lee KL, et al: Prognostic indicators from radionuclide angiography in medically treated patients with coronary artery disease. *Am J Cardiol* 53:18–22, 1984
3. Gal R, Grenier RP, Carpenter J, et al: High count rate first-pass radionuclide angiography using a digital gamma camera. *J Nucl Med* 27:198–206, 1986
4. Scholz PM, Rerych SK, Moran JF, et al: Quantitative radionuclide angiocardiography. *Cathet Cardiovasc Diag* 6:265–283, 1980
5. Ashburn WL, Schelbert HR, Verba JW: Left ventricular ejection fraction—A review of several radionuclide angiographic aprpoaches using the scintillation camera. *Prog Cardiovasc Dis* 20:267–284, 1978
6. Schelbert HR, Verba JW, Johnson AD, et al: Nontraumatic determination of left ventricular ejection fraction by radionuclide angiocardiography *Circulation* 51:902–909, 1975
7. Kennedy JW, Baxley WA, Figley MM, et al: Quantitative angiocardiography. I. The normal left ventricle in man. *Circulation* 34:272, 1966
8. Marshall RC, Berger HJ, Costin JC, et al: Assessment of cardiac performance with quantitative radionuclide angiocardiography. Sequential left ventricular ejection fraction, normalized left ventricular ejection rate, and

regional wall motion. *Circulation* 56:820–829, 1977
9. Basilico FC, Folland ED, Karaffa S, et al: Non-invasive measurmeent of left ventricular function in coronary artery disease. Comparison of first pass radionuclide ventriculography, M-mode echocardiography, and systolic time intervals. *Br Heart J* 45:369–375, 1981
10. Steele P, Kirch D, Matthews M, et al: Measurement of left heart ejection fraction and end-diastolic volume by a computerized, scintigraphic technique using a wedged pulmonary arterial catheter. *Am J Cardiol* 34:179–186, 1974
11. Folland ED, Hamilton GW, Larson SM, et al: The radionuclide ejection fraction: A comparison of three radionuclide techniques with contrast angiography. *J Nucl Med* 18:1159–1166, 1977